EFFECTS OF CHEMICAL COMPOSITION ON MECHANICAL PROPERTIES OF Al-Mg-Si-Mn BASED ALLOYS

Olena Prach[1], Oleksandr Trudonoshyn[2], Maxim Puchnin[3,*]

[1] Technische Universität Darmstadt, Alarich-Weiss-Straße 2, D-64287 Darmstadt, Germany
[2] Friedrich-Alexander-Universität Erlangen-Nürnberg, Martensstraße 5, 91058 Erlangen, Germany
3 Czech Technical University in Prague, Karlovo náměstí 13, 12135, Prague 2, Czech Republic

[*]corresponding author: e-mail: maxim.puchnin@fs.cvut.cz

Resume
Effects of chemical composition and heat treatment on the microstructural and mechanical properties of cast Al-Mg-Si-Mn alloys were investigated. The as-cast and heat treated alloys were investigated by microhardness, macrohardness and tensile stress measurements, scanning and transmission electron microscopy, energy dispersive X-ray analysis and differential scanning calorimetry. It was observed that the mechanical properties depend strongly on composition and addition of excess elements and eutectic phase. Heat treatment leads to the enhancement of all mechanical properties of alloys, which are the result of several mechanisms.

Article info
Article history:
Received 28 November 2016
Accepted 24 January 2017
Online 3 March 2017

Keywords:
Al-Mg-Si-Mn alloys;
Mg excess;
Si excess;
Microstructure;
Mechanical properties.

Available online: http://fstroj.uniza.sk/journal-mi/PDF/2017/02-2017.pdf

ISSN 1335-0803 (print version)
ISSN 1338-6174 (online version)

1. Introduction

Interest in heat treatable Al-Mg-Si aluminum alloys has been on the rise due to the ability to modify alloy hardness and thereby improve mechanical properties. The hardening effects arises as a result of interacting dislocations with the precipitates, which act as obstacles to the dislocation motion [1, 2]. It is well known that the ductility of such alloys decreases with increasing Si content and the brittle coarse Si particles usually make further deformation difficult [3].

Nevertheless, it is not only important to apply heat treatment conditions, but also to determine the optimal chemical composition of the material. The structure of Al-Mg-Si alloys consists of such phases as: solid solution of α-Al, primary Mg_2Si crystals and eutectic of Al-Mg_2Si.

An excess of Mg can decrease the solubility of Mg_2Si in the α-Al and obviously increases strength of materials after heat treatment [4, 5]. An excess of Mg in the Al-Mg_2Si system moves the eutectic point to a lower Mg_2Si concentration. It has also been shown that excess Mg in Al-Mg_2Si alloys can promote the formation of primary Mg_2Si and show that increasing Mg content decreases the volume fraction of the α-Al matrix and increases the volume fraction of Al-Mg_2Si eutectic phase [6 - 9].

An excess of Si significantly affects the diffusion of Mg and Si in Al liquid and produces α–Al dendrite structures. Increase of Si excess in the Al-Mg_2Si-Si composites leads to an increase of the solidification range. The aspect ratio of eutectics and size of primary particles are decreased with the increase of Si content in Al-Mg_2Si composites [10]. Also, excess Si has a positive effect on the properties of alloys after heat treatment. Authors [11, 12] show positive effect with subsequent heat

treatment on tensile stress alloys with excess Si. In the works [12, 13] beneficial action after aging on hardness and microhardness as well is shown. However, simultaneous modifications of chemical composition and heat-treatment and their effect on the mechanical properties of Al-Mg-Si alloys have not yet been investigated.

The main task of the paper is to elucidate influence of chemical composition on the mechanical properties and structure of Al-Mg-Si-Mn alloys. This investigation was performed through an examination of microstructural properties, including chemical composition at the micro-scale, as well as macroscopic measurements of mechanical properties, providing an understanding of the behavior of these alloys across several length scales

2. Materials and methods

The present article follows an earlier research of Al-Mg-Si alloys [14, 15]. The chemical compositions of evaluated alloys are represented in Table 1.

All alloys were prepared in an electric resistant furnace using graphite crucibles. High purity aluminum (A99.997), AlMg50, AlSi25 and AlMn26 were used as master alloys. The melt with the temperature (720 ± 5) °C had been degassed under argon atmosphere during 10 minutes.

Two types of heat treatment were applied. The first type was a solution treatment (in an electrical resistance furnace) and quenching in water at room temperature. The second type of heat treatment is T6, which combines solution treatment at 570 °C (60 min.), quenching in water and artificial aging at 175 °C over a variety of times.

Hardness was measured by a Universal testing machine (EMCOTEST M4C 075/750) with a ball diameter of 2.5 mm and a load of 62.5 kg, time of loading was 10 sec. Microhardness tests were carried out on polished non-etched specimens on a LECO M-400-G1 microhardness tester, HV0.05 with a standard indentation time. Tensile tests were carried out using testing machine (INSTRON 5582, USA), according to the standard EN ISO 6892-1.

Samples for microstructure observations in scanning electron microscope (SEM) were prepared using conventional metallographic techniques. The composition of the phases was measured by EDX analysis using SEM (JEOL JSM-7600F High Resolution Scanning Electron Microscope with EDS analysers (Oxford INCA Energy 250, UK), Japan) with accelerating voltage of 15 kV. To minimise the influence from the interaction volume during the EDX quantification, five point analyses on selected particles were conducted for each phase and the average was taken as the measurement.

Table 1

Nominal composition of alloys, wt. % (Al – bal.).

Elements	**Alloys**						
	M3	**MS1**	**MS2**	**M59**	**MS3**	**MS4**	**MS5**
Mg	6.0	7.0	7.0	5.0	7.0	7.0	7.0
Si	0.4	1.0	2.0	2.0	3.0	4.0	5.0
Mn	0.6	0.6	0.6	0.6	0.6	0.6	0.6
Expected Mg_2Si content	1Mg_2Si-5Mg	3Mg_2Si-5Mg	6Mg_2Si-3Mg	6Mg_2Si-1Mg	9Mg_2Si-1Mg	10.5Mg_2Si-0.5Si	10.5Mg_2Si-1.5Si

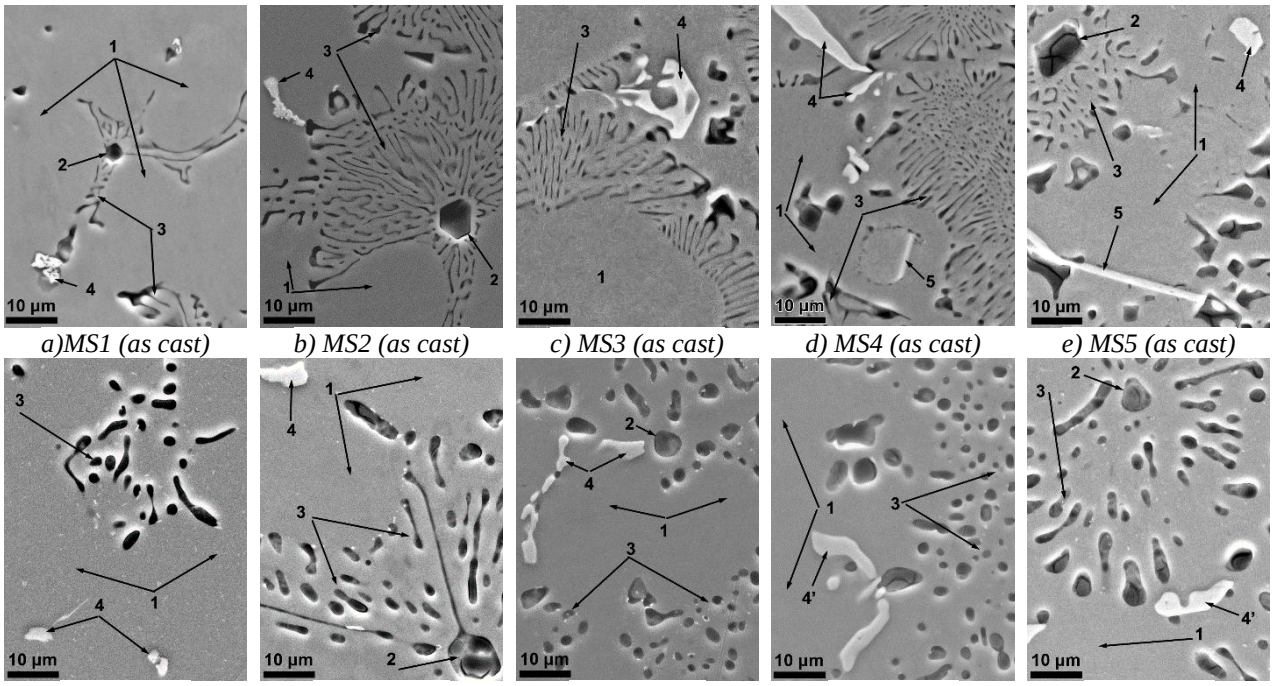

a)MS1 (as cast) *b) MS2 (as cast)* *c) MS3 (as cast)* *d) MS4 (as cast)* *e) MS5 (as cast)*

f) MS1 (HT) *g) MS2 (HT)* *h) MS3 (HT)* *i) MS4 (HT)* *j) MS5 (HT)*

Fig. 1. Microstructure of Al-7Mg-XSi-0,6Mn alloys: a) - e) as cast, f) - j) after heat treatment.

Table 2

Average composition of α-Al solid solution in alloys measured by EDX.

Alloy		Mg/Si ratio	Chemical composition, wt.%					
			O	Mg	Al	Si	Mn	Fe
M3	AC*	15.0	0.9	5.4	93.0	-	0.6	0.1
	HT**		0.8	5.6	92.9	-	0.	0.1
MS1	AC	7.0	0.9	4.4	94.8	0.2	0.6	0.1
	HT		0.9	5.8	92.6	0.1	0.6	-
MS2	AC	3.5	1.1	3.0	95.0	0.3	0.6	-
	HT		1.1	3.7	94.5	0.1	0.6	-
MS59	AC	2.5	0.7	1.9	96.6	0.3	0.5	-
	HT		0.6	1.9	96.7	0.3	0.5	-
MS3	AC	2.2	0.9	2.4	95.7	0.4	0.5	0.1
	HT		1.0	2.4	95.6	0.4	0.5	0.1
MS4	AC	1.8	1.1	2.0	95.9	0.5	0.5	-
	HT		0.8	0.9	97.1	0.7	0.5	-
MS5	AC	1.4	1.0	1.7	95.9	0.8	0.5	0.1
	HT		1.3	0.8	96.0	1.4	0.5	-

** - as-cast condition, ** - alloy after heat treatment*

3. Results and discussion

Microstructure and elements distribution. Fig. 1 represents the polished microstructure of samples. All alloys exhibit equiaxial grain structure. The following phases constituents can be distinguished based on the results of EDX analysis:

1. Matrix of α-Al (light areas);

2. Primary Mg_2Si crystals (black);

3. Eutectic of Al-Mg_2Si (dark-grey areas);

4. Manganese phases $Al_6(Mn,Fe)$, α-$Al_{15}(Mn,Fe)_3Si_2$;

4'. Mangan-silicon phase β-$Al_5(Mn,Fe)Si$;

5. Silicon-manganese phase δ-$Al_4Si_2(Mn,Fe)$;

In the present series of alloys, Mg and Si content in solid solution changes with alteration of the Mg/Si ratio in alloys (Table 2). Mg is considered in excess when the ratio is more than 2, and excess of Si - less than 2. For all

alloys Mn content in α-Al solid solution is 0.5 - 0.6 wt. % (Table 2). Existence of an insignificant peak of oxygen in EDX-spectrum is explained by tendency of Al and Mg2Si to oxidation. The average composition of α-Al matrix for all samples is represented in Table 2.

Homogenization equalizes the distribution of all elements in the grain and increases the excess element (Mg or Si) in α-Al matrix (Table 2). Exceptions are M59 and MS3 alloys, in which the concentration of the Mg and Si in solid solution changes slightly. It can depend on Mg/Si ratio, which is close to stoichiometric in these alloys.

Mn- and Si-containing phases. Due to the presence of iron in the Mn ligature which have poor solubility in Al-Mg-Si alloys, we observe the formation of acicular-shaped intermetallic inclusions of high Fe and Si content, which reduce the strength and ductility of the alloys. To neutralize the negative effect of the Fe-containing phase [12 - 16], investigated alloys are additionally doped by 0.6 % Mn.

In alloy with the nominal composition of Al-7Mg-5Si wt. %, two eutectics (Al-Mg_2Si and Al-Si) are formed [12]. However, the eutectic Al-Si was not detected in the alloy with a nominal composition Al_7Mg_5SiMn (Fig. 1 j and 4 d). Therefore an excess of silicon with manganese and iron form several types of manganese phase in submitted alloys.

As it is shown by further studies, the addition of 0.6 wt. % of manganese in the alloy with nominal composition Al-7Mg-3Si improves its mechanical properties. Thus tensile strength and yield strength of the alloy with manganese addition increases on average by 30 %.

The morphology of primary Mn-containing phase observed in all alloys is shown in Fig. 1. Its chemical composition and stoichiometry are represented in Table 3. These phases can be identified as $Al_6(Mn,Fe)$, α-$Al_{15}(Mn,Fe)_3Si_2$, β-$Al_5(Mn,Fe)Si$, δ-$Al_4(Mn,Fe)Si_2$. As it can be seen from Fig. 1 and Table 3, heat treatment promotes the transformation of metastable phases to stable conditions [16 - 18].

Eutectic. An overview of the thermal effects in the investigated alloys and therefore theirs melting point can be obtain from the DSC curves. The experiments were conducted in alloys with different Mg and Si content. Fig. 2a shows the curves of the changes in the heat flow depending on the temperature for the MS2, M59 and MS3 alloys. In the temperature range from 20 – 590 °C no thermal effects were observed. When the temperature reaches close to 590° C on the all of heating curve, a negative thermal effect occurs, which corresponds to an endothermic reaction. The first endothermic effect can be attributed to the melting of the eutectic (Al) + (Mg_2Si) and starts at T = 594 ± 3 °C. The second heat effect corresponds to the melting of α-Al matrix. As it can be seen, amount of the eutectic (Al) + (Mg_2Si) as well as excess of Mg does not significantly effect on the behavior of alloys during heating. Peaks corresponding to the melting of Mn-containing phases have not been detected due to a small amount. Therefore, we can judge, that the initial melting point of alloys of Al-Mg-Si is the melting point of (Al) + (Mg_2Si) eutectic - 594° C.

Another situation occurs in alloys with excess of Si that can be seen on Fig. 2b. In MS4 and MS5 alloys, in comparison with other studded alloys, new peaks were detected. They start close to 570°C and merge with the peak of (Al) + (Mg_2Si) eutectic. Due to [17, 18] they can be classified as a melting of Mn- and Si- containing phases. Thus, α-(AlFeSi) and β-(AlMnFeSi) phases have melting points in range 560-570 °C, (Al)-(Si) eutectic – 575° C and δ-(AlMnFeSi) – 596 °C. The temperatures of these reactions are close to each other and to identify them on the DSC curves it is necessary to use more precise equipment.

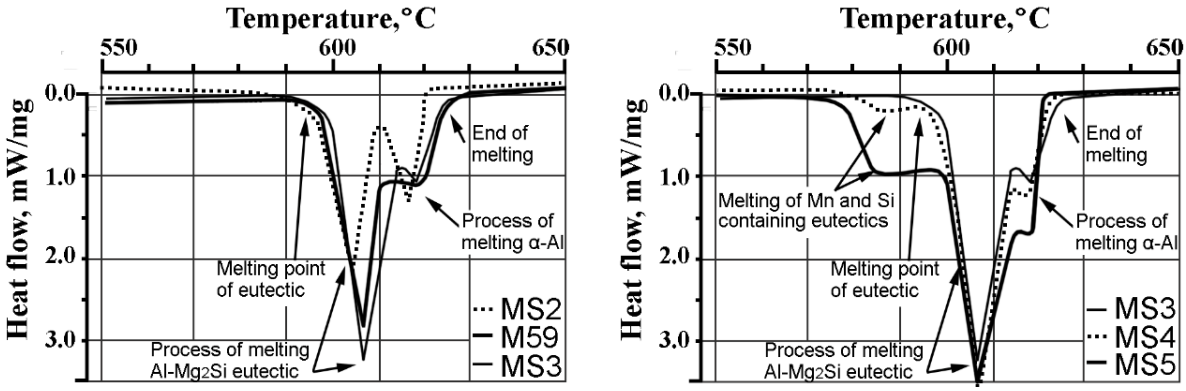

a) MS2, M59, MS3 alloys *b) MS3, MS4, MS5 alloys*

Fig. 2. Comparison DSC curves of MS2, M59, MS3 (a) and MS3, MS4, MS5 (b) alloys (cooling rate 10 K/min).

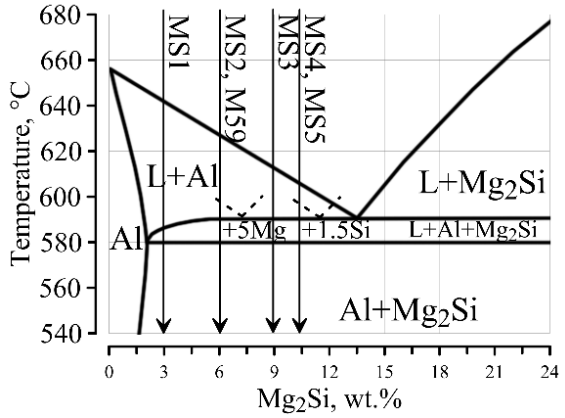

Fig. 3. Equilibrium phase diagrams of Al-Mg_2Si system.

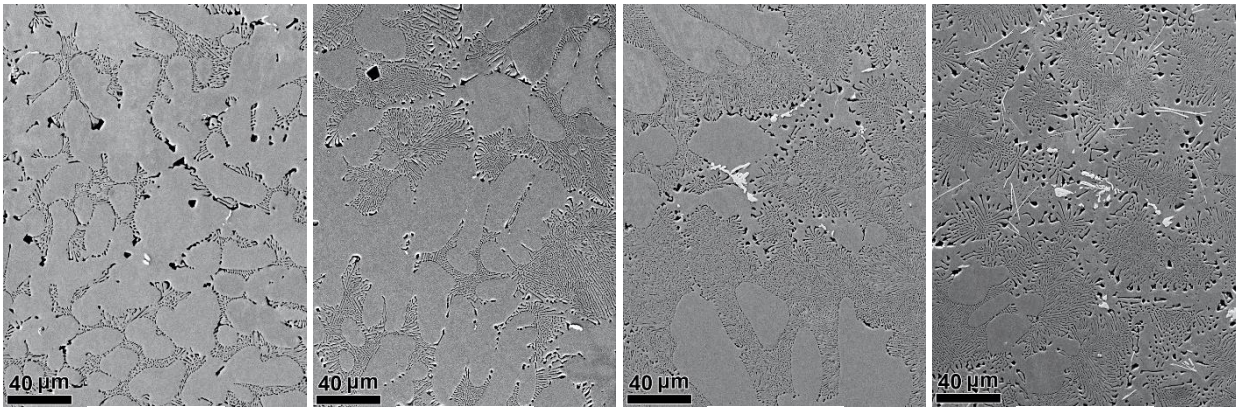

a) M59 alloy *b) MS2 alloy* c) *MS4 alloy* d) *MS5 alloy*

Fig. 5. Volume fraction of Al-Mg2Si eutectic in: a) M59 alloy, b) MS2 alloy, c) MS4 alloy, d) MS5 alloy dependency on Mg and Si content.

With the addition of Mg into the Al-Mg_2Si system, the eutectic point moves towards the corner with lower Mg_2Si concentration (Fig. 3), the volume of primary α-Al decreases with increasing of the Al-Mg_2Si eutectic volume (Fig. 4 a, b). As it was mentioned in [21], the Al-Mg_2Si eutectic volume fraction grows with the increase of Mg_2Si in the Al-Mg_2Si alloys.

Increase of excess of Si in the Al-Mg2Si alloys leads the eutectic point to higher Al concentration and decrease of the volume of primary α-Al and increase of the Al-Mg_2Si eutectic volume. In MS5 alloy with 1.5 wt. % excess of Si, primary α-Al practically disappears, and the volume fraction of Al-Mg_2Si

eutectic reaches maximum (Fig. 4 c,d).

Mechanical properties. The results of hardness and tensile tests are summarized in Fig. 5. As the result of solution treatment both macrohardness (HB) and microhardness (HV0.05) values are significantly decreasing (except MS5 alloy). Artificial aging leads to an increase in all mechanical properties of the investigated alloys. Changing during heat treatment is the result of several processes, which simultaneously occurs during heating.

The first process is the eutectic spheroidization. The higher solution treatment temperature leads to faster eutectic lamella decomposition into smaller segments and to a spheroidizing effect [15]. This process (according to the results as presented on Fig. 5) leads to a decrease in the hardness of the alloys.

The second process is dissolution of primary Mn-containing phases and the formation of dispersoids, which include Mn, Si and Fe. These particles can be identified as α-($Al_{15}(Mn,Fe)_3Si_2$) phase [21, 22]. Absence of coherence of phase α-($Al_{15}(Mn,Fe)_3Si_2$) with α-Al probably affects the decrease of the hardness of the alloys, (along with disintegration of eutectic cells). Also, the dissolution of the β'-Mg_9Si_5 particles occurs during homogenization.

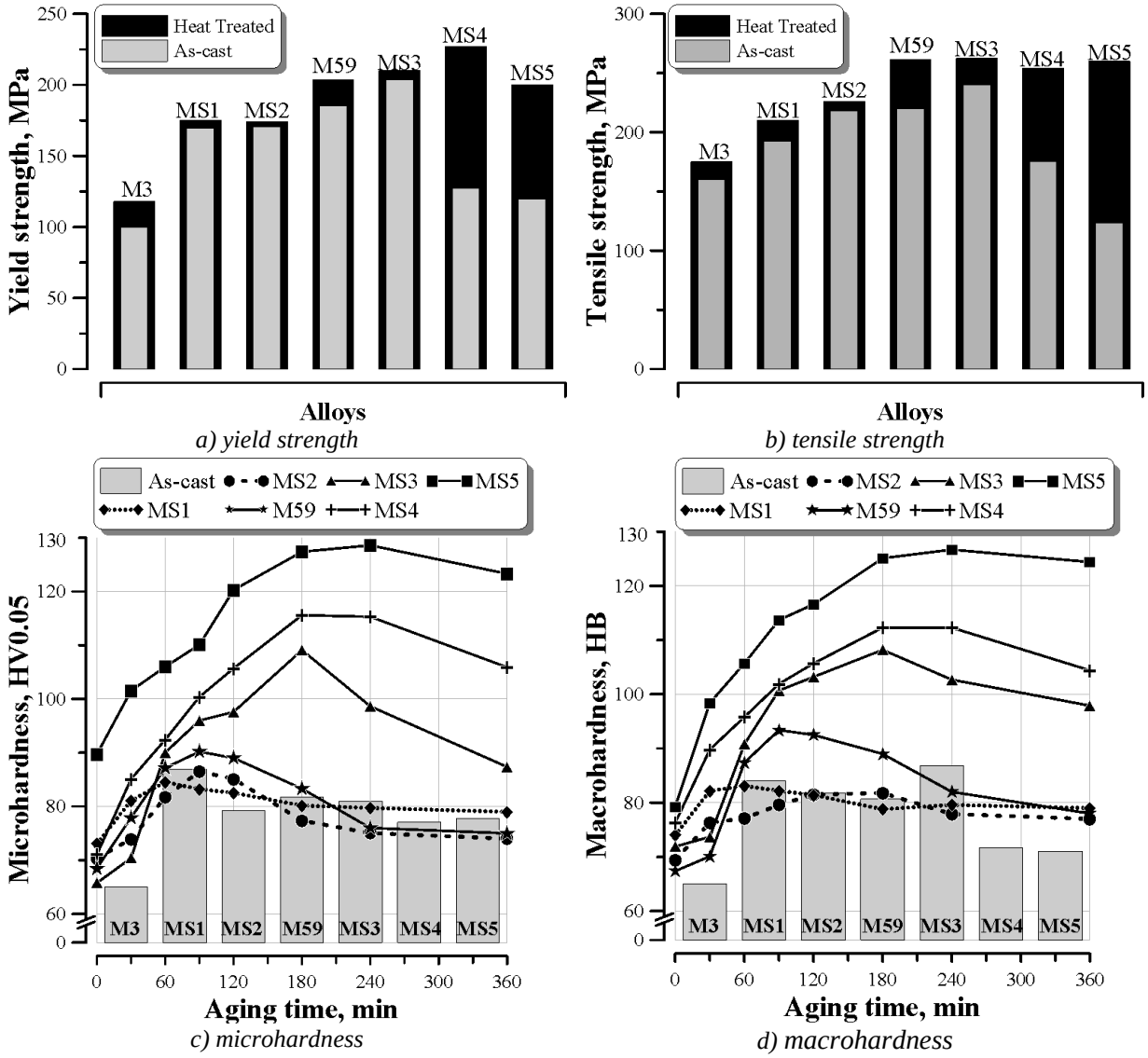

Fig. 5. Mechanical properties of MS-series.

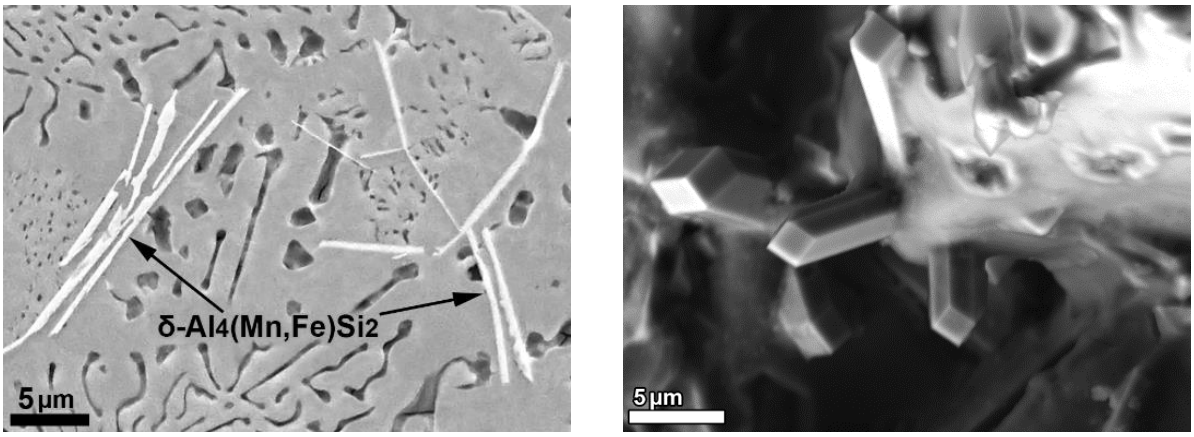

a) microsection *b) deep etched*

Fig. 6. Morphology of needle-shaped polyhedral δ-Al4(Mn,Fe)Si2 phase in MS5 alloy.

Table 3

Average composition of Mn-containing phases measured by EDX.

Phase name	Alloy	Chemical composition, wt.%						
		O	Mg	Al	Si	Mn	Fe	Cu
Al_6(Mn,Fe) (blocky-shaped)	M3	1.4	0.8	73.2	0.1	16.1	8.3	0.1
	MS1	1.6	1.8	70.7	1.1	16.2	8.5	0.1
	MS2 (AC)	2.1	2.2	70.4	1.0	16.4	7.8	0.1
α-Al_{15}(Mn,Fe)$_3Si_2$, (blocky-shaped, stable phases)	MS2 (HT)	0.9	0.6	65.6	5.5	17.8	9.4	0.2
	M59 (AC)	1.8	0.9	70.5	5.5	13.2	7.8	0.3
	M59 (HT)	1.0	1.1	70.7	5.8	13.5	7.5	0.4
	MS3 (AC)	1.7	0.7	66.5	4.9	14.3	11.3	0.6
	MS3 (HT)	1.5	0.7	69.7	4.8	13.3	9.9	0.1
δ-Al_4(Mn,Fe)Si_2 (acicular-shaped)	MS4 (AC)	1.5	1.1	60.4	26.8	7.6	2.2	0.4
	MS5 (AC)	1.1	0.7	58.1	21.3	16.8	1.7	0.3
β-Al_5(Mn,Fe)Si (blocky-shaped, stable phase)	MS5 (AC)	0.5	0.2	59.2	11.9	25.1	2.4	0.7
	MS4 (AC)	0.8	0.6	62.0	10.4	21.8	4.0	0.4
	MS4, MS5 (HT)	1.6	1.00	63.5	11.6	21.9	2.3	0.1

The last process occurs in alloy MS4, MS5 is transformation of metastable acicular-shaped δ-phases (Fig. 6) to more stable state due to the diffusion processes [23, 24]. After solution treatment the excess of Si from the δ-phase dissolves in α-aluminum solid solution (Tables 2, 3). As it can be seen from Fig. 6c this process is confirmed by the results from microhardness tests.

Hardness and tensile strength of the cast Al-Mg_2Si alloys do not increase with the growth of Mg content (MS2 and M – alloys with same volume of Mg_2Si and different values of Mg), but can relate to the size and morphology of the eutectic and primary Mg_2Si phases (M3 and MS1, M59 and MS3 – alloys with same the value of Mg and different volume of Mg_2Si), it can be seen from Fig. 5. Similar results were obtained in the works [6, 11].

The alloys of Al-Si-Mg system with increase of Mg content up to a certain quantity leads to increase of mechanical properties, but further increase of the Mg content leads to decrease of mechanical properties [25]. As can be seen from the graphs (Fig. 5), heat treatment does not affect on the mechanical properties (both of hardness and tensile strength) of alloys with extra magnesium. Also, heat treatment of alloys with extra silicon improves the mechanical properties. With increasing time of artificial aging (at 175 °C) the hardness of alloys with extra silicon grows.

It can be explained by a sufficient amount of silicon in solid solution to form a larger number of strengthening particles.

Fractography analysis. Insignificant hardening effect on alloys with extra magnesium content was confirmed by results of fractography analysis. Behavior of the fracture surface also confirms that the main strengthening phase in the studded system is the Al-Mg_2Si eutectic. With increase of the eutectic amount the percentage of brittle surfaces proportional increases, thereby tensile strength become higher (from the quasi-viscous MS1 to transgranular MS3).

Initiation of destruction is on the line of the eutectic cells – α-matrix grains and eutectic cells – eutectic cells (alloys M59, MS2, MS3). Additional stress concentrations (in alloys MS4 and MS5) are caused by the presence of elongated acicular-shaped inclusions (δ-phase). This confirms our assumption that the cause of the sharp deterioration of mechanical properties in the as-cast state is silicon-containing particles. The dendrites of α-matrix behave similar to grains and strong interaction between inclusions and slip bands, which generates at the grain boundaries during the plastic deformation process [26]. The final fracture paths tend to pass through the eutectic cells and the fracture of eutectic generates the formation of flat areas (Fig. 7). The fracture path preferentially goes through the shrinkage porosity in the case of the existence of excessive shrinkage defects, which results in the significant decrease of mechanical properties [27].

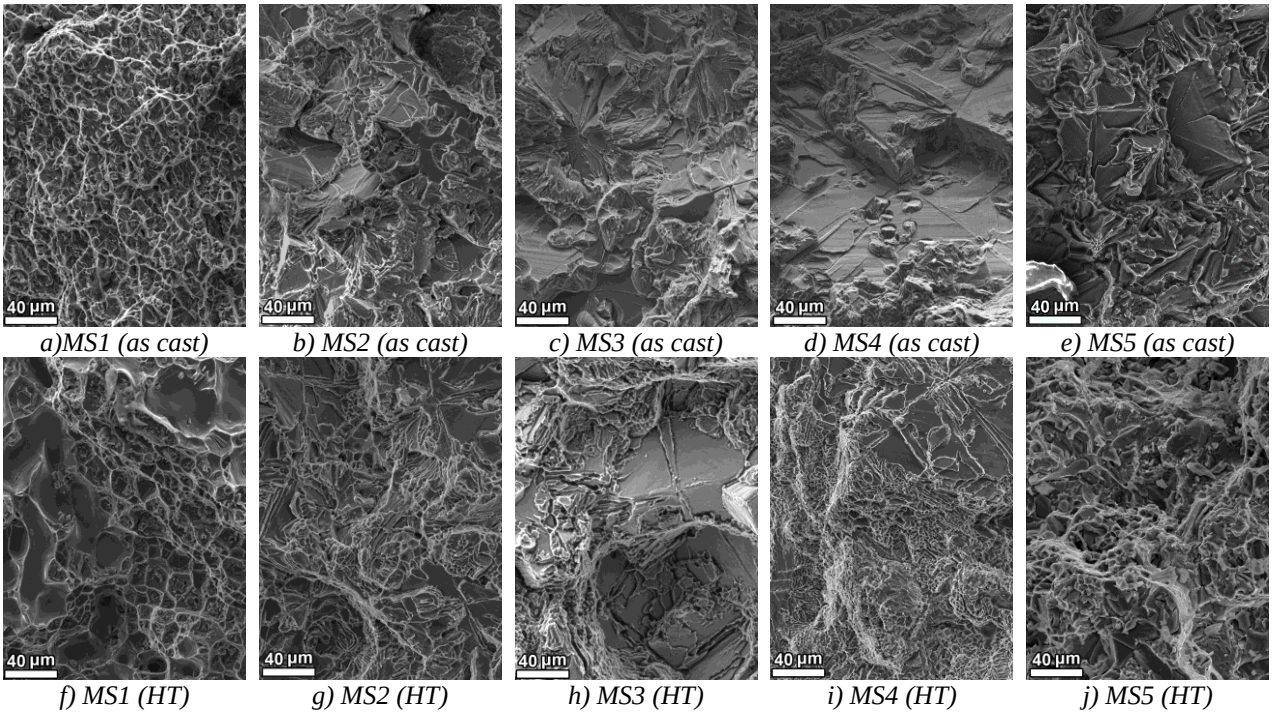

a)MS1 (as cast) *b) MS2 (as cast)* *c) MS3 (as cast)* *d) MS4 (as cast)* *e) MS5 (as cast)*

f) MS1 (HT) *g) MS2 (HT)* *h) MS3 (HT)* *i) MS4 (HT)* *j) MS5 (HT)*

Fig. 7. Fractography of Al-7Mg-XSi-0,6Mn alloys: a) - e) as cast, f) - j) after heat treatment.

Solution treatment leads to the quantity reduction of brittle surfaces compared with the cast condition and the formation of a viscous fracture. This is associated with spheroidization of the eutectic lamellas. It confirms decrease of mechanical properties that we can see on the graphs of hardness. Similar effect of heat treatment on the formation of the fracture surface was obtained by the author [27].

4. Conclusions

Increase of Si content leads to the formation of less stable phases. In alloys with an excess of Si metastable δ-$Al_4(Mn,Fe)Si_2$ phases are

formed. This leads to the degradation of mechanical properties. It has been found that the an excess of silicon (MS4 and MS5 alloys) promote the formation of strengthening particles in α-matrix during aging, which leads to appreciable increase of tensile strength.

The higher solution treatment temperature leads to faster eutectic lamella decomposition into smaller segments and to spheroidizing effect.

Homogenization equalizes distribution of all elements in grain and increases the excess element (Mg or Si) in α-Al matrix and transformation of metastable silicon-manganese acicular-shaped δ-phase to more stable state (α or β) due to diffusion processes.

Excess magnesium did not have a meaningful effect on the mechanical properties of alloys.

The main strengthening phase in the studded system is the eutectic cells of Al-Mg_2Si.

Acknowledgements

The authors thank our colleagues Prof. K. Mykhalenkov and V. Boyko for the provision of alloys for research and participation in discussions, although they may not agree with all of the conclusions of this paper. The authors also thank the Chair Metallic Materials TU-Berlin, where alloys for this study were melted.

This research was supported by the Visegrad Fund (V4EaP) and the German Academic Exchange Service (DAAD).

This work was supported by the Ministry of Education, Youth and Sport of the Czech Republic, program NPU1, project No LO1207.

References

[1] N. Fridlyander, V.G. Sister, O.E. Grushko, V.V. Berstenev, L.M. Sheveleva, L.A. Ivanova:. Metal Science and Heat Treatment 44(9) (2002) 365-370.

[2] S. Zajac, B. Bengtsson, C. Jonsson: Mater. Sci. Forum 396-402 (2002) 399-404.

[3] Y. Wang, H. Liao, Y. Wu, J. Yang: Materials and Design 53 (2014) 634–638.

[4] C. Li, Y. Wu, H. Li, X. Liu: Journal of Alloys and Compounds 477 (2009) 212–216.

[5] J. Zhang, Z. Fan, Y. Q. Wang, B. L. Zhou: Mater. Sci. Technol. 17 (2001) 494-496.

[6] F. Yan, S. Jib, Z. Fanc: Mater. Sci. Forum 765 (2013) 64-68.

[7] A. Furihata, K. Matsuda, J. Nakamura, S. Ikeno, Y. Uetani: Mater. Sci. Forum 519-521 (2006) 507-510.

[8] A. Radziszewska: Journal of Microscopy 237(3) (2010) 384–387.

[9] K. Matsuda, T. Yoshida, T. Wada, A. Yoshida, U. Uetani, T. Sato, A. Kamio, S. Ikeno: J. Japan Inst. Metals 62 (1998) 718-726.

[10] J. Zhang, Y. Wang, B. Yang: J. Mater. Res. 14(1) (1999) 68-74.

[11] J. Qingxiu, Z. Caixia, H. Xiaodong: China Foundry 6(2) (2009) 133-136.

[12] E. Georgatis, A. Lekatou, A.E. Karantzalis, H. Petropoulos, S. Katsamakis, A. Poulia: J. Mater. Eng. Perform. 22(3) (2013) 729-741.

[13] L. C. Doan, K. Nakai, Y. Matsuura, S. Kobayashi, Y. Ohmori: Materials Transactions, 43(6) (2002) 1371-1380.

[14] M. Puchnin, O. Trudonoshyn, O. Prach: Mater. Tehnol. 50(2) (2016) 247–252.

[15] O. Trudonoshyn, M. Puchnin, O. Prach: Mater. Tehnol. 50(3) (2016) 427–431.

[16] Z. Zhihao, M. Yi, C. Jianzhong: China Foundry 9(4) (2012) 349-355.

[17] L. Lia , R. Zhoua, D. Lua, Y. Jianga, R. Zhoua: Materials Research 17(2) (2014) 511-517.

[18] C. Phongphisutthinan, H. Tezuka, T. Sato: Materials Transactions 52(5) (2011) 834-841.

[19] L.F. Mondolfo. Aluminium Alloys: Structure and Properties. Butterworth & Co Publishers Ltd; 2nd Revised edition, December 1979.

[20] N. A. Belov, D.G. Eskin, A.A. Aksenov. Multicomponent phase diagrams: applications for commercial aluminum alloys. Elsevier, 2005.

[21] S. Otarawanna, C.M. Gourlay, H.I. Laukli, A.K. Dahle: Metallurgical And Materials Transactions A 40A (2009) 1645-1659.

[22] L. Lodgaard, N. Ryum: Mater. Sci. Eng. A283

(2000) 144–152.

[23] G.A. Edwards, K. Stiller, G.L. Dunlop, M.J. Couper: Acta Mater. 46(11) (1998) 3893-3904.

[24] C. Ravi, C. Wolverton: Acta Mater. 52 (2004) 4213–4227.

[25] L. Hong, S. Wen-Ju, Z. Gang, L. Chun-Ming, Z. Liang: Trans. Nonferrous Met. Soc. China 15(1) (2005) 30-31.

[26] J. Wen-Ming, F. Zi-Tian, L. De-Jun, Microstructure: Trans. Nonferrous Met. Soc. China 22 (2012) 7−13.

[27] G. Mrówka-Nowotnik: Archives of Materials Science and Engineering 46(2) (2010) 98-107.